

Adsorption Reactions of Dimethylaluminum Isopropoxide and Water on the H/Si(100)-2 × 1 Surface: Initial Reactions for Atomic Layer Deposition of Al₂O₃

Manik Kumer Ghosh and Cheol Ho Choi*

Department of Chemistry, College of Natural Sciences, Kyungpook National University,
Taegu 702-701, South Korea

Received: January 17, 2006; In Final Form: March 29, 2006

The surface reaction pathways of dimethylaluminum isopropoxide (DMAI) and water with the H/Si(100)-2 × 1 surface were theoretically investigated with SIMOMM:MP2/6-31G(d). The oxygen atom in DMAI stabilizes an initial complex, facilitating the approach of DMAI to the surface. The methane loss reaction, propane loss reaction, methylation, hydrogen loss reaction, and ring closing reaction channels of the DMAI–surface reactions were identified. Among these, the methane loss reaction depositing –Al(CH₃)OCH(CH₃)₂ was found to be the major channel due to low barrier height and large exothermicity. The ring closing reaction is kinetically the second most accessible channel, even though it is not thermodynamically favorable. On the basis of these theoretical results, recent experimental data were reinterpreted such that the experimentally observed peaks of CH₄ and CH(CH₃)₂OH are in fact the products of these two channels. The propane loss reaction is kinetically the third most probable channel. It produces the surface Si–O bond, which is a reaction unique to DMAI as compared to trimethylaluminum. In summary, the oxygen substitution not only affects the basic nature of the existing potential energy surfaces but also opens new possibilities.

I. Introductions

Atomic layer deposition (ALD) is a film deposition technique that is based on the sequential use of self-terminating gas–solid reactions.¹ It is usually applied in areas where fabrication of a thin layer of film requires precision control of thickness and conformal structure.^{2,3} Atomic level control in ALD film growth is achieved through a sequence of chemical reactions in which the saturating surface reactions ideally limit the growth to one monolayer per cycle.⁴

In the semiconductor industry, SiO₂ is widely used as a standard gate dielectric layer. However, continued miniaturization in accordance with “Moore’s Law” will render SiO₂ unusable as a gate oxide layer within a decade due to the quantum tunneling effect.⁵ Therefore, research for alternative materials to replace SiO₂ has been critical in recent years.⁶ The most promising alternative dielectric materials are the high- κ binary metal oxides. If a higher dielectric constant material, for example, Al₂O₃, HfO₂, or ZrO₂, is used as the gate dielectric, then the tunneling problem can be avoided.⁷ Among these, aluminum oxide is one of the most promising SiO₂ replacement materials due to its relatively high dielectric constant ($\kappa \approx 9$) compared to SiO₂ ($\kappa \approx 3.9$) and large band offset with silicon.^{8,9} Furthermore, its thermal and chemical stability allows its application as a good diffusion barrier material.^{7,10}

Various aluminum halide, alkyl, and alkoxide precursors, such as AlCl₃, AlBr₃, AlMe₂Cl, AlMe₃, AlEt₃, Al(OEt)₃, and Al(O^{*i*}-Pr)₃ have been employed with oxygen sources, O₂, O₃, H₂O, H₂O₂, etc. for the growth of Al₂O₃ thin films of high quality at reduced temperatures in both ALD and chemical vapor deposition (CVD) processes.^{1,11,12} There have been some theoretical studies of the chemical processes related to the Al₂O₃ ALD. Musgrave and co-workers¹³ carried out a density functional

theory (DFT) study of trimethylaluminum (TMA), AlCl₃, and H₂O ALD half-reactions with small gas-phase Al(OH)_{*n*}(CH₃)_{*m*} clusters. Yamashita and co-workers¹⁴ studied the reactions between dimethylaluminum and a model H/Si(111) surface with DFT. Halls and Raghavachari¹⁵ studied the reactions of TMA and H₂O with the H/Si(100)-2 × 1 surface.

To avoid formation of an interfacial SiO₂ layer caused by the oxidation of Si substrate during the supply of the oxygen source, there have been studies where aluminum alkoxides are used as an oxygen source.^{2,3} Among various precursors, aluminum alkoxides contain an oxygen atom that can itself be the oxygen source. In addition, alkoxides are easy to prepare and purify and are intrinsically noncorrosive. Recently, An et al.¹⁶ experimentally performed the atomic layer deposition of Al₂O₃ using dimethylaluminum isopropoxide (DMAI) and water (H₂O). They reported an atomically flat and uniform Al₂O₃ film that is comparable to those obtained by the TMA–H₂O ALD process.

Despite these studies, the role of oxygen in DMAI is still not certain. Atomistic understandings of the underlying reactions of various precursors give us control over these surface reactions that eventually lead to a technique to tailor the ALD.¹⁷ In the present work, as a model system of aluminum alkoxides, an extensive theoretical study of the potential energy surfaces of reaction mechanisms is performed to elucidate the initial adsorption mechanisms of DMAI and water precursors on the H/Si(100)-2 × 1 surface.

II. Computational Details

To obtain the energetics of adsorption reactions of DMAI and H₂O precursors, electronic structure calculations based on second-order Moller–Plesset perturbation theory (MP2) were performed using a cluster model of the Si(100) surface. All calculations reported here were performed with the general

* Author to whom correspondence should be addressed. Phone: +82-53-950-5332. Fax: +82-53-950-6330. E-mail: cchoi@knu.ac.kr.

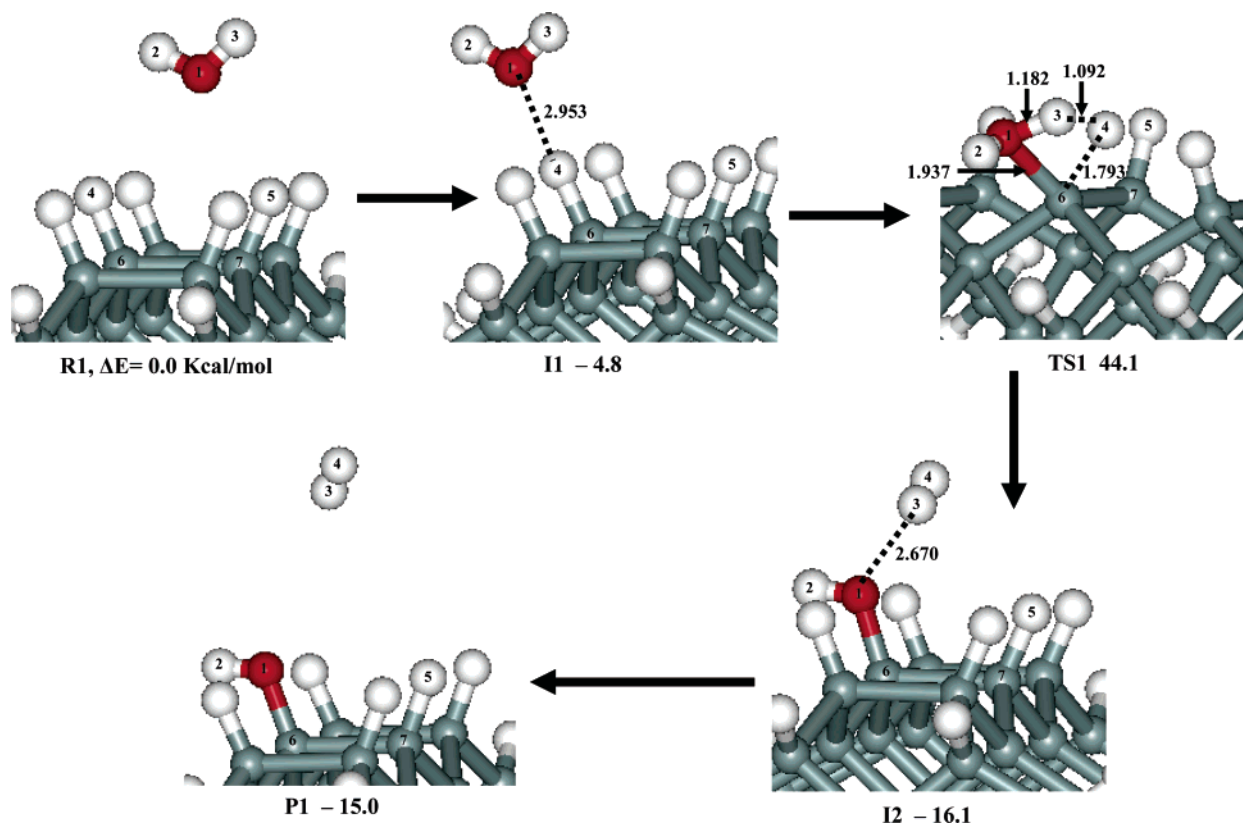
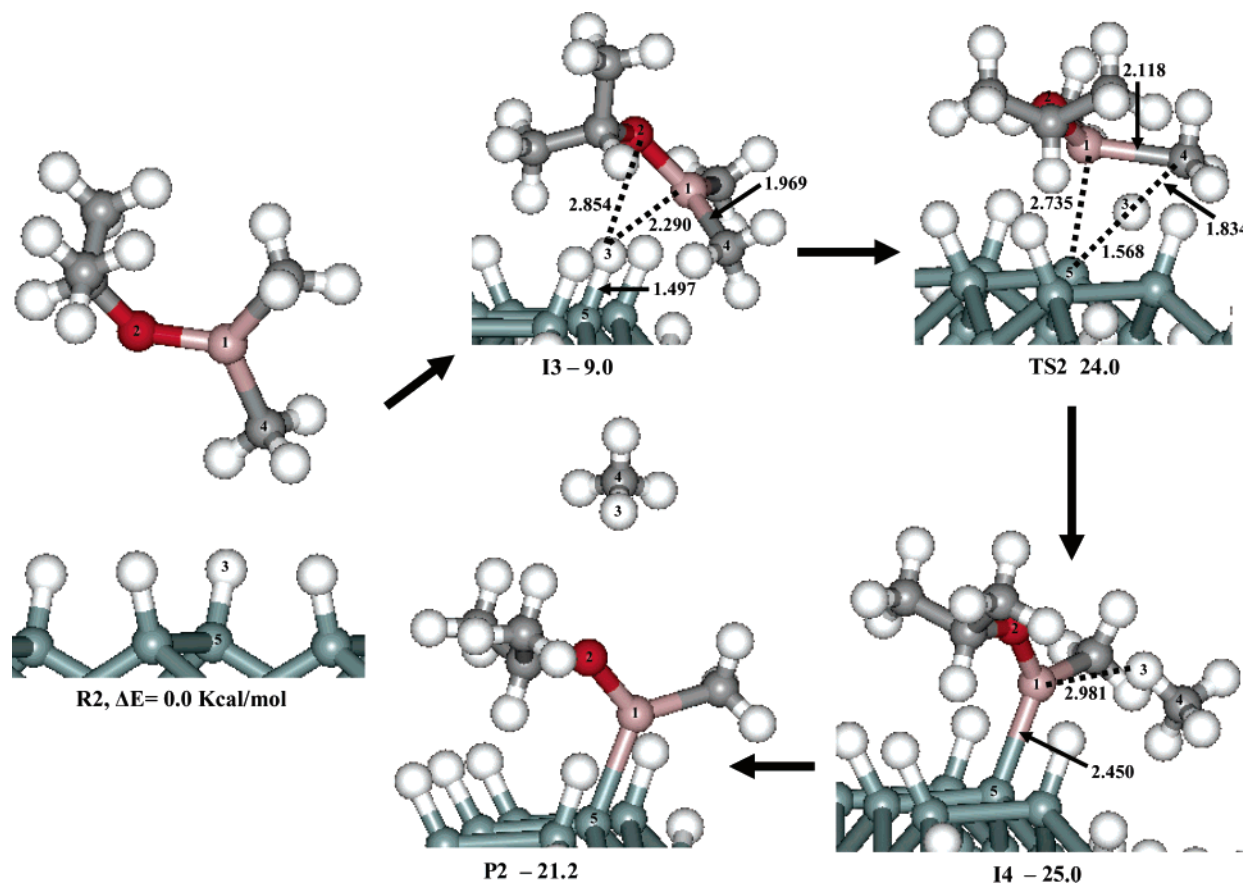
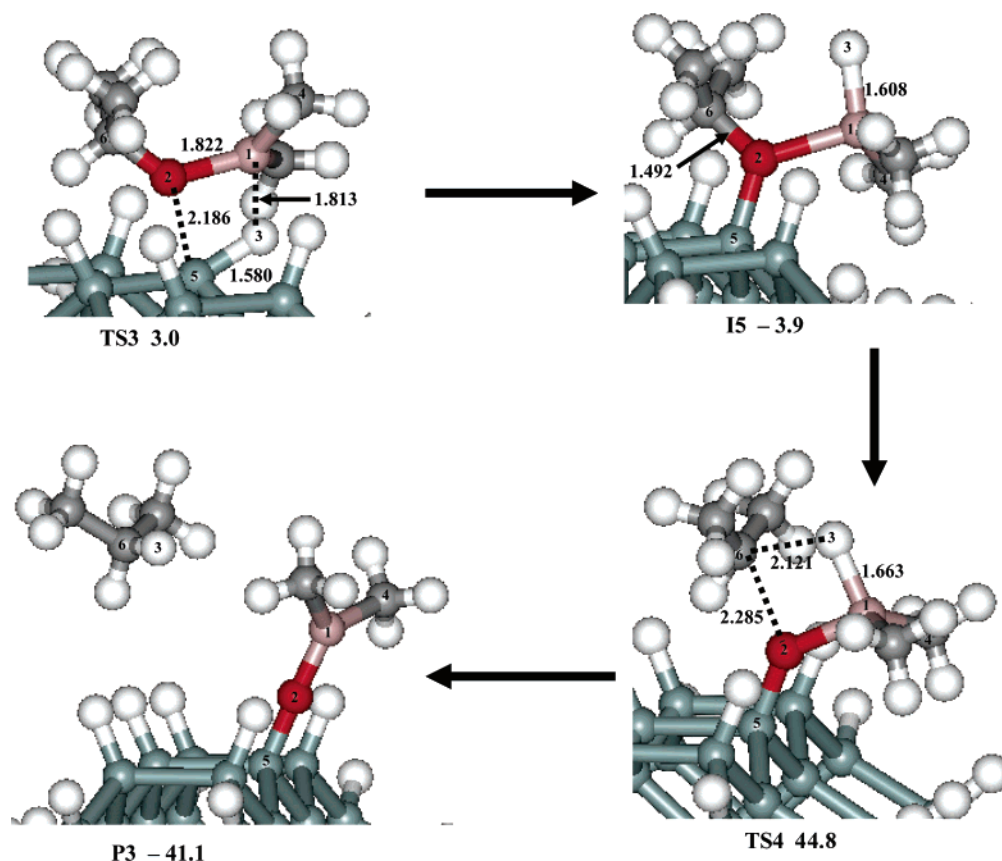
CHART 1: Stationary Points along the Initial Water Adsorption on the H/Si(100)-2 × 1 Surface as Calculated with SIMOMM:MP2/6-31G(d)^a^a The bond distances are in angstroms, and the energies are in kcal/mol.**CHART 2: Stationary Points along the Methane Loss Reaction of DMAI on the H/Si(100)-2 × 1 Surface as Calculated with SIMOMM:MP2/6-31G(d)^a**^a The bond distances are in angstroms, and the energies are in kcal/mol.

CHART 3: Stationary Points along the First Channel of the Propane Loss Reaction of DMAI on the H/Si(100)-2 × 1 Surface as Calculated with SIMOMM:MP2/6-31G(d)^a

^a The bond distances are in angstroms, and the energies are in kcal/mol.

atomic and molecular electronic structure system (GAMESS) electronic structure program.¹⁸ An all-electron 6-31(d)¹⁹ basis set was used through this work. Minimum energy reaction paths were determined by first optimizing the geometries of the minimum and the transition states. The Hessian matrix (matrix of energy second derivatives) was computed and diagonalized for all stationary points to characterize them. Intrinsic reaction coordinate (IRC) calculations, using the Gonzalez–Schlegel second-order method,²⁰ were conducted to verify that each saddle point connects minima of interest.

To study surface size effects, a hybrid quantum mechanics/molecular mechanics (QM/MM) method called SIMOMM was adopted.²¹ The chemically inactive region of the system is calculated by computationally inexpensive force field methods, while the chemically active part is treated by quantum mechanics. It has been shown that the surface integrated molecular orbital molecular mechanics (SIMOMM) QM/MM method gives reasonable results at relatively low computational cost.¹⁷ In this work, the QM/MM models were designed such that OSi₉H₁₆ and AlOC₅Si₉H₂₇ quantum regions are embedded in OSi₄₈H₄₄ and AlOC₅Si₄₈H₅₇ clusters for water and DMAI studies, respectively. These two models have one and three surface Si dimer(s) in the QM and MM regions, respectively. MM3²² parameters were used for the molecular mechanics part of the computations. All of the computations were done without imposing symmetry unless otherwise specified.

III. Results and Discussions

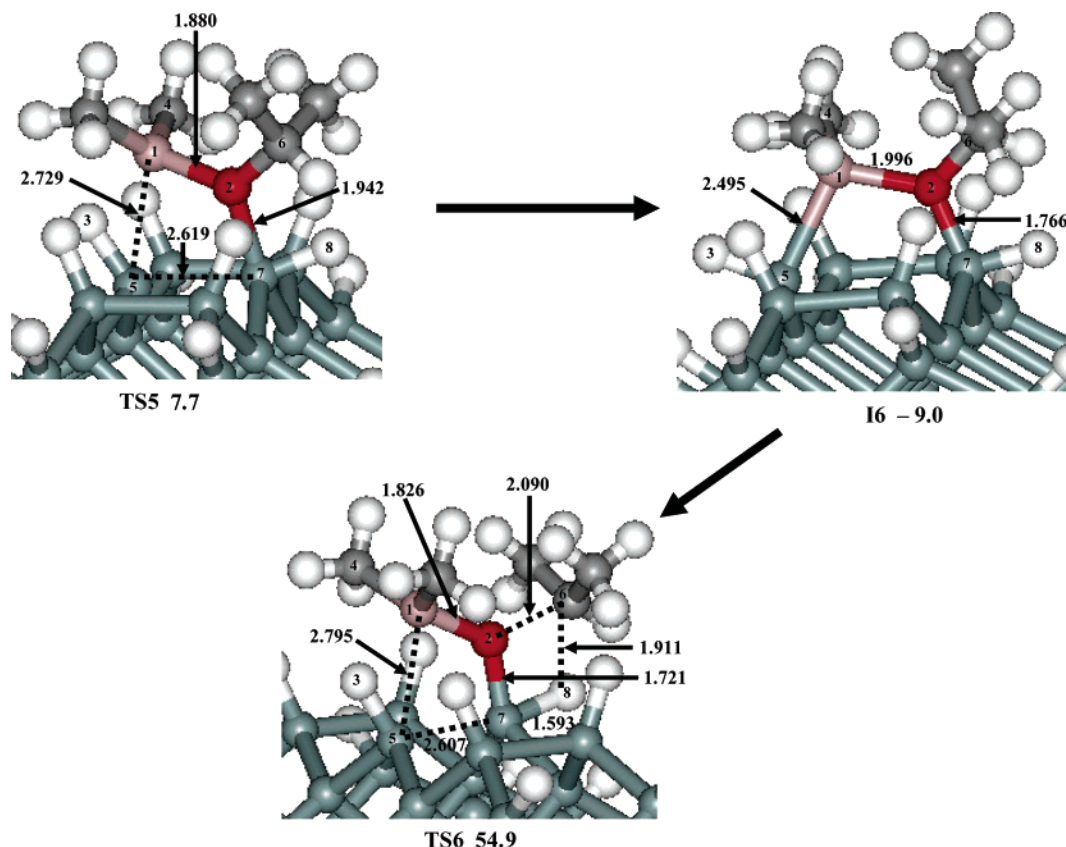
A. Reaction between H₂O and the H/Si(100)-2 × 1 Surface. Previously, Halls and Raghavachari (HR)¹⁵ extensively studied the water adsorption reaction with the help of B3LYP/dzdp.

They studied both hydroxylation and H/D exchange reactions and found that the former is the preferred pathway. The hydroxylation reaction was investigated in the current study, and the results are presented in Chart 1. In the surface hydroxylation pathway, H₂O reacts with the H/Si(100)-2 × 1 surface and forms the Si–O linkage by releasing a hydrogen molecule.

The initial complex **I1** shows a weak interaction between O1 and H4 with a stabilization energy of 4.8 kcal/mol. The distance of O1–H4 is 0.42 Å shorter than that of HR, which may be due to the deficiency of DFT in the description of weak interactions. In the process of forming the surface Si–O bond, the transition state **TS1** connects **I1** and another intermediate **I2** with an overall barrier height of 44.1 kcal/mol. It is seen that the leaving H₂ molecule is making a weak bond with O2 in the intermediate **I2**, which was not reported by HR. The final product **P1** is formed by releasing H₂ with slight endothermicity from **I2**. The overall reaction enthalpy is exothermic by 15.0 kcal/mol, which is very close to HR's value (15.9 kcal/mol).¹⁵ In general, our overall reaction pathway closely resembles that of HR¹⁵ except for some minor details.

B. Reactions between DMAI and the H/Si(100)-2 × 1 Surface. Unlike TMA, DMAI has both Al and O atoms that can act as a nucleophile producing surface Si–O and Si–Al bonds. According to our calculations, four initial reaction and one subsequent reaction pathways of DMAI adsorption on the H/Si(100)-2 × 1 surface were found, which are discussed in order. Note that the asterisks indicate surface species.

Reaction 1: Si–H* + DMAI → Si–Al(CH₃)–O–CH(CH₃)₂* + CH₄. A methane loss reaction yields a surface Si–Al bond and free methane. The detailed reaction pathway is presented

CHART 4: Stationary Points along the Second Channel of the Propane Loss Reaction of DMAI on the H/Si(100)-2 × 1 Surface as Calculated with SIMOMM:MP2/6-31G(d)^a

^a The bond distances are in angstroms, and the energies are in kcal/mol.

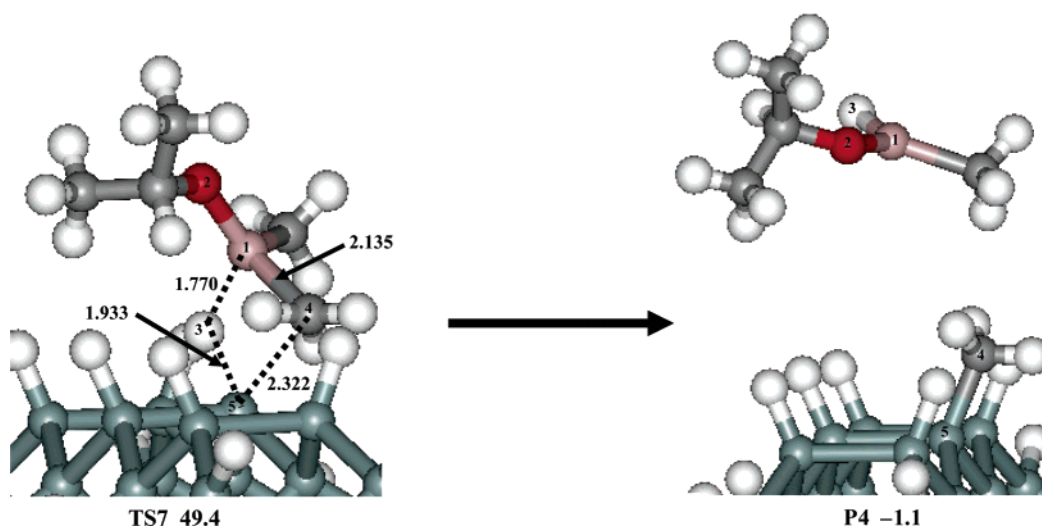
in Chart 2. As DMAI approaches the surface, it forms a complex, **I3**. The distances of Al1–H3 and O2–H3 are calculated to be 2.29 and 2.85 Å, respectively, showing that both Al1 and O2 are interacting with the surface H3. The stabilization energy of **I3** is calculated to be 9.0 kcal/mol, which is 4.2 kcal/mol larger than that of **I1**. Likewise, **I3** is about 9 kcal/mol more stable than the relevant initial complex of TMA adsorption,¹⁵ where only the Al–H-type interaction exists. Therefore, it is clear that the oxygen in DMAI greatly facilitates the initial approach of precursor to the surface. **TS2**, where Al1 is making a bond with Si5 and H3 is migrating from Si5 to C4, connects **I3** and another intermediate **I4** with an overall barrier height of 24.0 kcal/mol, which is similar to that (28.1 kcal/mol) of TMA. **I4** is an intermediate with a weak interaction between Al1 and H3. Since O2 does not directly participate in bond forming and bond breaking of **TS2**, it is understandable that the relevant barriers of DMAI and TMA are similar. The overall reaction enthalpy is calculated to be 21.2 kcal/mol exothermic, which is more exothermic than that of TMA by 12.2 kcal/mol. In short, the oxygen in DMAI is playing an important role in the initial part of the adsorption reaction and the thermodynamic stabilization of the product **P2**.

Reaction 2: $\text{Si-H}^* + \text{DMAI} \rightarrow \text{Si-O-Al}(\text{CH}_3)_2^* + \text{CH}_3\text{CH}_2\text{CH}_3$. A propane loss reaction produces a surface Si–O bond and a free propane, which is a unique reaction of the DMAI precursor. Two reaction pathways were found leading to the loss of propane. They are presented in Charts 3 and 4, respectively. Both pathways start from the initial complex **I3**. However, unlike the methane loss reaction, the O2 is acting as a nucleophile making a bond with Si5. At the same time, Al1 is abstracting H3 forming a unique four-membered ring in **TS3** with a very mild reaction barrier of 3.0 kcal/mol. **TS3** connects

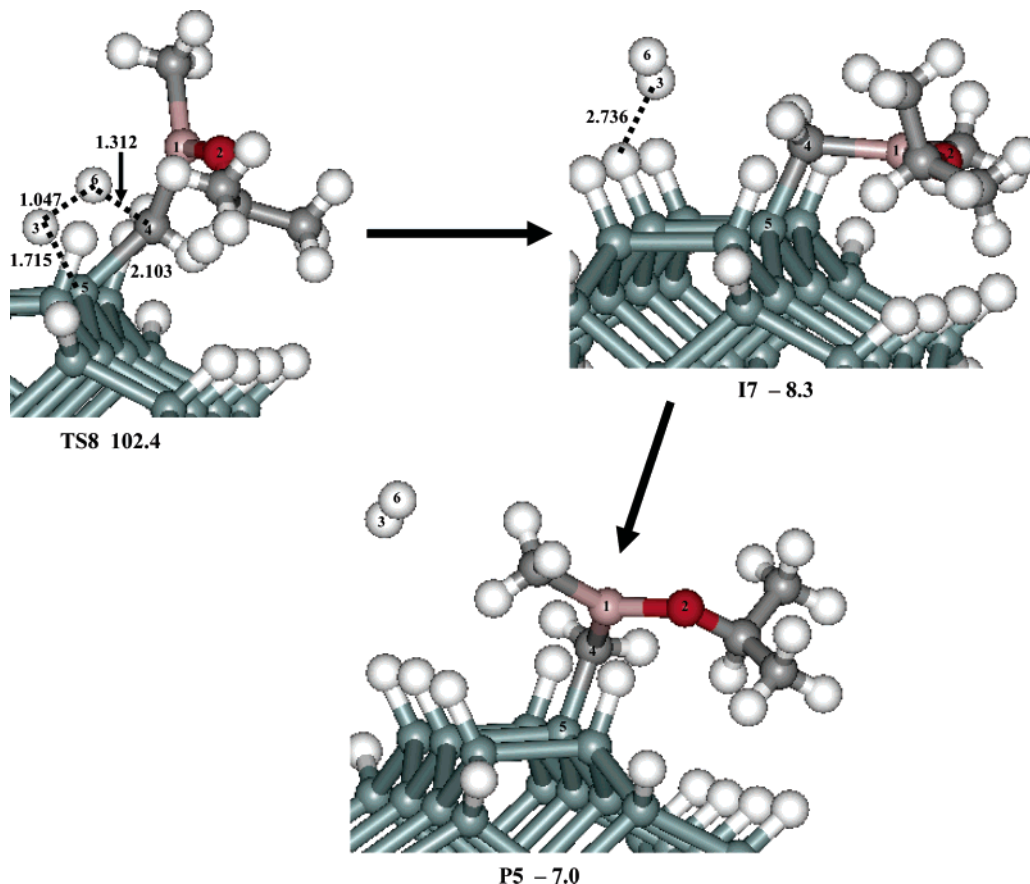
complex **I3** and an intermediate **I5**, which has an unfavorable trivalent O2 and a tetravalent Al1. As a result, **I5** is even less stable than **I3**. To form the final product **P3**, the reaction passes through another transition state **TS4**, where H3 is migrating to C6 and the O2–C6 bond is being broken with a barrier height of 44.8 kcal/mol. The final product has a unique surface Si–O–Al(CH₃)₂ bonding with an overall stabilization energy of 41.1 kcal/mol. Even though the exothermicity of the propane loss reaction is larger than that of the methane loss reaction by 19.9 kcal/mol, it is kinetically much less favorable due to its larger barrier height.

An alternative pathway starts from the same initial complex **I3** (Chart 4). Transition state **TS5** connects **I3** and an intermediate **I6** with an overall barrier height of 7.7 kcal/mol. In **TS5**, both O2 and Al1 are making bonds with Si7 and Si5, respectively. As in **I5**, the resulting intermediate **I6** has energetically less favorable trivalent O2 and tetravalent Al1, making it less stable than **I3**. By forming the Si5–Si7 bond and migrating H8 to C6, the transition state **TS6** connects **I6** and the product **P3** with an overall barrier of 54.9 kcal/mol, which is 10.1 kcal/mol higher than that of **TS4**, making this channel kinetically much less accessible than the first pathway.

Reaction 3: $\text{Si-H}^* + \text{DMAI} \rightarrow \text{Si-CH}_3^* + \text{H-Al}(\text{CH}_3)_2\text{-O-CH}(\text{CH}_3)_2$. A surface methylation reaction is another possible channel (Chart 5). Again **I3** is the starting point of this reaction. As DMAI approaches the surface as shown in **TS7**, it transfers a methyl group to the surface while abstracting a H3 from it. The overall reaction barrier and the reaction enthalpy are calculated to be 49.4 and –1.1 kcal/mol, respectively. These values show that methylation is both kinetically and thermodynamically less probable than the propane loss reaction (reaction 2). The overall barrier height is calculated to be 16.9

CHART 5: Stationary Points along the Methylation of DMAI on the H/Si(100)-2 × 1 Surface as Calculated with SIMOMM:MP2/6-31G(d)^a

^a The bond distances are in angstroms, and the energies are in kcal/mol.

CHART 6: Stationary Points along the Hydrogen Loss Reaction of DMAI on the H/Si(100)-2 × 1 Surface as Calculated with SIMOMM:MP2/6-31G(d)^a

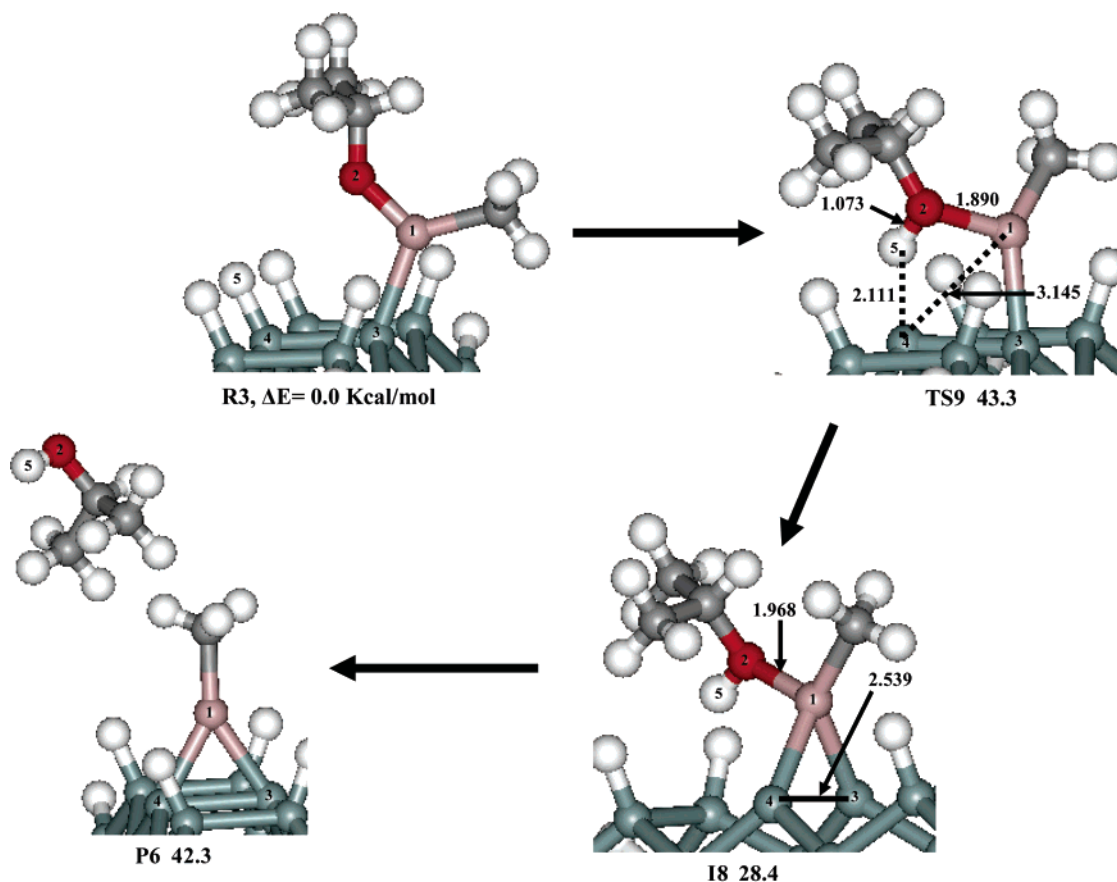
^a The bond distances are in angstroms, and the energies are in kcal/mol.

kcal/mol higher than that of the relevant reaction of TMA¹⁵ showing that the oxygen atom in DMAI makes the methylation reaction difficult to occur. It is reasonable to assume that the electron withdrawing effect of O₂ reduces the reactivity of AlI yielding the higher reaction barrier.

Reaction 4: $\text{Si-H}^* + \text{DMAI} \rightarrow \text{Si-CH}_2\text{Al}(\text{CH}_3)\text{-O-CH}(\text{CH}_3)_2^* + \text{H}_2$. A hydrogen loss reaction is another possible channel yielding the surface Si5-C4 bond (Chart 6). According to our calculations, this has the highest reaction barrier of all

reactions considered here. The transition state **TS8** connects **I3** and a complex **I7** with a barrier height of 102.4 kcal/mol, which is 10.6 kcal/mol higher than the relevant barrier of TMA adsorption.¹⁵ Even though the overall reaction enthalpy is calculated to be 7.0 kcal/mol exothermic, the large barrier nearly prohibits this channel from being activated under normal conditions.

Reaction 5: Ring Closing Reaction Producing CH(CH₃)₂OH. Once **P2** is formed in the methane loss reaction, it can further

CHART 7: Stationary Points along the Ring Closing Reaction of DMAI on the H/Si(100)-2 × 1 Surface as Calculated with SIMOMM:MP2/6-31G(d)^a

^a The bond distances are in angstroms, and the energies are in kcal/mol.

undergo a ring closing reaction as shown in Chart 7. **TS9** connects **R3** (note that **R3** corresponds to **P2** without CH_4) and an intermediate **I8** with a barrier height of 43.3 kcal/mol. During the ring closing, Al1 nucleophilically attacks Si4 while O2 abstracts H5. As in **I5** and **I6**, the intermediate **I8** has thermodynamically unfavorable trivalent O2 and tetravalent Al1, making it less stable than **R3** by 28.4 kcal/mol. By breaking Al1–O2 of **I8**, the final product **P6** is formed without a transition state. Overall endothermicity of the ring closing reaction is as large as barrier height. Therefore it is not a thermodynamically favorable reaction. However, considering the fact that experiments were done in nonequilibrium conditions, the final products would be mostly determined by the kinetic factors. If so, since the overall barrier height of this channel is lower than those of reactions 2, 3, and 4, the surface product **P6** has a better chance of being formed.

C. Experimental Considerations. To elucidate the reaction mechanism, An et al.¹⁶ performed experiments with a model pulse sequence of the DMAI– H_2O ALD process. They monitored the reaction products by a quadrupole mass analyzer. The signals of $m/z = 16$ (CH_4) and 60 ($\text{CH}(\text{CH}_3)_2\text{OH}$) were detected when DMAI alone was pulsed. They interpreted these peaks as being due to the limited mass resolution and/or imperfect pumping of the residual gases in the reactor. However, according to our calculations, it is very likely that the peaks correspond to the products of reactions 1 and 5, respectively. The fact that these two channels have the lowest reaction barriers among the DMAI adsorption pathways identified in this study further supports our conclusions.

IV. Conclusions

The surface reaction pathways of dimethylaluminum isopropoxide (DMAI) and water with the H/Si(100)-2 × 1 surface were theoretically investigated, focusing on the effect of the oxygen atom in DMAI. Initial reaction complexes exist both in water and in DMAI reaction pathways. The oxygen in DMAI further stabilizes the initial complex as compared to the relevant complex of TMA adsorption. The methane loss reaction, propane loss reaction, methylation, hydrogen loss reaction, and ring closing reaction channels of the DMAI–surface reactions were identified. The ring closing and propane loss channels are the unique reactions of DMAI, which do not exist in TMA adsorptions. Among these, the methane loss reaction is predicted to be the major channel due to the low barrier height and large exothermicity. The ring closing reaction can be kinetically the second most accessible channel. On the basis of these two probable reactions, we reinterpreted the previous experimental observations and concluded that the peaks of CH_4 and $\text{CH}(\text{CH}_3)_2\text{OH}$ can be in fact the products of these two channels. Since the overall barrier height of the propane loss channel is only slightly higher than that of the ring closing reaction, it can also occur. Further experimental studies are expected.

In summary, the oxygen in DMAI participates in various parts of potential energy surfaces. It facilitates the initial approach of DMAI to the surface and allows the propane loss reaction and ring closing reaction to occur.

Acknowledgment. This work was supported by the Korea Research Foundation (Grant No. KRF-2005-070-C00065).

References and Notes

- (1) Ritala, M.; Leskelä, M. In *Handbook of Thin Film Materials*; Nalwa, H. S., Ed.; Academic Press: San Diego, CA, 2001; Vol. 1, Chapter 2.
- (2) Ritala, M.; Kukli, K.; Rathu, A.; Räsänen, P. I.; Leskelä, M.; Sajavaara, T.; Leinonen, J. *Science* **2000**, 288, 319.
- (3) Leskelä, M.; Ritala, M. *Thin Solid Films* **2002**, 409, 138.
- (4) Heyman, A.; Musgrave, C. B. *J. Phys. Chem. B* **2004**, 108, 5718–5725.
- (5) Muller, D. A.; Sorsch, T.; Moccio, S.; Baumann, F. H.; Evans-Lutterodt, K.; Timp, G. *Nature* **1999**, 399, 758.
- (6) Packan, P. A. *Science* **1999**, 285, 2079.
- (7) Wilk, G. D.; Wallace, R. M.; Anthony, J. M. *J. Appl. Phys.* **2001**, 89, 5243.
- (8) Klein, T. M.; Niu, D.; Epling, W. S.; Li, W.; Maher, D. M.; Hobbs, C. C.; Hedgw, R. I.; Baumvol, I. J. R.; Parsons, G. N. *Appl. Phys. Lett.* **1999**, 25, 4001.
- (9) Manchanda, L.; Morris, M. D.; Green, M. L.; van Dover: R. B.; Klemens, F.; Sorsch, T. W.; Silverman, P. J.; Wilk, G.; Busch, B.; Aravamudan, S. *Microelectron. Eng.* **2001**, 59, 351.
- (10) Copel, M.; Cartier, E. P.; Gusev, S.; Guha, S.; Bojarczuk, N.; Poppeller, M. *Appl. Phys. Lett.* **2001**, 78, 2670.
- (11) Suntola, T. In *Handbook of Crystal Growth*; Hurler, D. T. J., Ed.; Elsevier Science: New York, 1994; Vol. 3, pp 605–663.
- (12) Puurunen, R. L. *J. Appl. Phys.* **2005**, 97, 121301.
- (13) (a) Widjaja, Y.; Musgrave, C. B. *Appl. Phys. Lett.* **2002**, 80, 3304. (b) Heyman, A.; Musgrave, C. B. *J. Phys. Chem. B* **2004**, 108, 5718.
- (14) Matsuwaki, T.; Nakajima, T.; Yamashita, K. *J. Phys. IV* **2001**, 11, 63.
- (15) (a) Halls, M. D.; Raghavachari, K. *J. Chem. Phys.* **2003**, 118, 10221–10226. (b) Halls, M. D.; Raghavachari, K.; Frank, M. M.; Chabal, Y. J. *Phys. Rev. B* **2003**, 68, 161302. (c) Halls, M. D.; Raghavachari, K. *J. Phys. Chem. B* **2004**, 108, 4058.
- (16) (a) An, K.; Cho, W.; Sung, K.; Lee, S. S.; Kim, Y. *Bull. Korean Chem. Soc.* **2003**, 24, 1659. (b) Cho, W.; Sung, K.; An, K.; Lee, S. S.; Chung, T.; Kim, Y. *J. Vac. Sci. Technol., A* **2003**, 21, 1366.
- (17) (a) Choi, C. H.; Gordon, M. S. *J. Am. Chem. Soc.* **1999**, 121, 11311. (b) Choi, C. H.; Gordon, M. S. *The Chemistry of Organic Silicon Compounds*; Rappoport, Z., Apeloig, Y., Eds.; John Wiley & Sons: New York, 2001; Vol. 3, Chapter 15, pp 821–852. (c) Choi, C. H.; Gordon, M. S. *Computational Materials Chemistry: Methods and Applications, Theoretical Studies of Silicon Surface Reactions with Main Group Absorbates*; Curtiss, L. A., Gordon, M. S., Eds.; Kluwer Academic Publishers: Norwell, MA, 2004; Chapter 4, pp 125–190.
- (18) (a) Schmidt, M. W.; Balbridge, K. K.; Boatz, J. A.; Elbert, S. T.; Gordon, M. S.; Jensen, J. H.; Koseki, S.; Matsunaga, N.; Nguyen, K. A.; Su, S.; Windus, T. L.; Dupuis, M.; Montgomery, J. A., Jr. *J. Comput. Chem.* **1993**, 14, 1347. (b) Fletcher, G. D.; Schmidt, M. W.; Gordon, M. S. *Adv. Chem. Phys.* **1999**, 110, 267.
- (19) Herhe, W. J.; Ditchfield, R.; Pople, J. A. *J. Chem. Phys.* **1972**, 56, 2257.
- (20) (a) Gonzalez, C.; Schlegel, H. B. *J. Phys. Chem.* **1990**, 94, 5523. (b) Gonzalez, C.; Schelegel, H. B. *J. Chem. Phys.* **1991**, 95, 5853.
- (21) Shoemaker, J. R.; Burgruff, L. W.; Gordon, M. S. *J. Phys. Chem. A* **1999**, 103, 3245.
- (22) (a) Allinger, N. L.; Yuh, Y. H.; Lii, J. H. *J. Am. Chem. Soc.* **1989**, 111, 8551. (b) Lii, J. H.; Allinger, N. L. *J. Am. Chem. Soc.* **1989**, 111, 8566. (c) Lii, J. H.; Allinger, N. L. *J. Am. Chem. Soc.* **1989**, 111, 8576.